Available online at www.sciencedirect.com
SCIENCE DIRECT
Polymer 46 (2005) 2978–2985
polymer
www.elsevier.com/locate/polymer

Exfoliated PA6,6 nanocomposites by modification with PA6

I. González, J.I. Eguiazábal, J. Nazábal*

Departamento de Ciencia y Tecnología de Polímeros and Instituto de Materiales Poliméricos 'POLYMAT', Facultad de Ciencias Químicas, UPV/EHU, P.O. Box 1072, 20080 San Sebastián, Spain

Received 5 July 2004
Available online 2 March 2005

Abstract

Minor amounts of a fully exfoliated PA6/commercial OMMT nanocomposite were used as a master-batch to produce exfoliated PA6,6 based nanocomposites. The major component PA6,6, which was fully mixed with PA6, did not largely affect the interactions between the OMMT and the surrounding polymer, as the exfoliation level of OMMT increased upon blending with PA6,6. Both the phase behaviour and the mechanical properties of the nanocomposites were compared with those of the PA6,6-rich matrix, to assess the separate effects of the PA6 and the OMMT. The large exfoliation level attained, led to increases in the modulus of elasticity that reached 46% with 5 wt% OMMT, and to the presence of highly ductile materials up to 3 wt% OMMT content.

Keywords: Nanocomposites; Polyamide 6,6; Master-batch

1. Introduction

It is known that the reinforcement at the nanoscale of a polymer by a layered silicate leads to nanocomposites that employing minimal silicate contents (<10 wt%) [1], improve the advantages in stiffness, strength, barrier properties, etc. that microcomposites offer with higher mineral contents. Moreover, this is without the disadvantage of decreases in fracture properties such as ductility and impact strength, and with the advantage of easier processing.

Nanoscale structures are obtained by exfoliation of modified layered mineral clays, mostly montmorillonite (MMT). In general, there are three main methods to obtain nanocomposites: monomer intercalation, solvent, and polymer melt intercalation [1]. Polymer melt intercalation is the preferred method, because the absence of solvents makes it environmentally sound and economically advantageous. Moreover, the process would be carried out in the usual processing equipment. However, exfoliation in the melt state is comparatively difficult [2]. The lack of knowledge that exists on the relation between the adequate chemical nature of the polymeric matrix and the organic modification of the MMT, and the often precarious thermal stability of the organic modification, account for this difficult exfoliation.

A wide exfoliation of the organically modified MMT (OMMT) was relatively easy in the case of polyamide 6 [3–8], and also in polymers such as polycaprolactone [9–10] and polyacrylates [11]. However, in most polymers, the polymer-OMMT interaction is not favourable enough to fully exfoliate the aluminosilicate platelets, leading to intercalated or partially exfoliated structures [12–13]. For this reason, a number of methods have been employed to help exfoliation become a widespread process. Among them, the use of chemically modified matrices to help interactions with the OMMT, for instance with maleic anhydride [14], the optimisation of processing conditions [4], or the addition of a polymer that would either interact or be miscible with both the OMMT and the matrix polymer [15–17] have been used.

In the case of PA6,6 significant exfoliation levels were observed using OMMTs synthesized in the laboratory [18–25]. Studies on crystal structure and thermal behaviour of nanocomposites [18], phase transition on annealing [19], spatial distribution of OMMT in the matrix [20], toughness [21] and molecular modelling techniques to predict binding energies [22] have been carried out. The introduction of

* Corresponding author. Tel.: +34 943 018218; fax: +34 943 015270.
E-mail address: popnaetj@sq.ehu.es (J. Nazábal).

0032-3861/$ - see front matter © 2005 Elsevier Ltd. All rights reserved.
doi:10.1016/j.polymer.2005.02.022

silicate layers induced the appearance of the γ crystalline phase in nanocomposites at room temperature, changed the structure of the α crystalline phase, increased the crystallization rate and had a strong heterophase nucleation effect on the PA6,6 matrix [18]. The mechanical properties increased by the addition of OMMT [23–25], but less than that seen in PA6 due to the lower exfoliation level. With respect to the organic modification used, the increases obtained in strength and modulus using co-intercalation of either epoxy resin and alkylammonium [23] or cetyltrimethylammonium bromide [25] were better than those obtained using octadecylammonium and aminoundecanoic acid [24]. However, when commercial OMMTs were used to produce PA6,6 nanocomposites, the improvements in mechanical properties were low and far from those attained in PA6/OMMT nanocomposites. This was because the interactions were not favourable and therefore only partial exfoliation of the clay was obtained.

The current search for a dispersed clay structure depends on both the interactions and the interfacial tension between the dispersed component and the matrix. This situation is similar to that which exists when a blend of two immiscible polymers is to be compatibilized. In this case, the addition of a third polymeric component; either partially miscible, or one that interacts or that reacts with the two components of the blends, has been used successfully [16–17,26–27]. This method has been used to produce nanocomposites based on PC [15], SAN [16] and PVC [17] and might be used in the case of other matrices where clay exfoliation is difficult. For instance, PA6 is both miscible in PA6,6, and able to exfoliate OMMT in the melt state. Therefore, it could be used to exfoliate OMMT and then produce PA6,6-rich nanocomposites by mixing with PA6,6 in two stages. A single extrusion [28] in a larger extruder might succeed by feeding the organoclay and PA6 to the hopper, while PA6,6 could be added at a downstream seed port.

In this work, we have tried to obtain melt processed PA6,6/OMMT nanocomposites using extruded PA6/OMMT exfoliated nanocomposites as a master-batch to produce PA6,6/PA6/OMMT nanocomposites rich in PA6,6. The morphologies obtained were analysed by X-ray diffraction (XRD), and transmission electron microscopy (TEM). The phase structure of the nanocomposites was characterized by dynamic mechanical analysis (DMTA) and differential scanning calorimetry (DSC), and the mechanical properties were measured by means of tensile and impact tests.

2. Experimental

The Polyamide 6,6 was Zytel® 101L (Dupont) and the Polyamide 6 was Durethan® B30S (Bayer). The filler was a natural surface-modified montmorillonite (Nanomer®, I.30TC, Nanocor Inc.) (OMMT). Drying before processing was performed at 90 °C in vacuo for 14 h for PA6,6 and PA6, and at 80 °C in an air-circulation oven for 4 h in the case of OMMT. The 90/10 wt/wt PA6/OMMT nanocomposite master-batch was obtained in a Collin ZK25 co-rotating twin-screw extruder-kneader. The diameter and length to diameter ratio of the screws were 25 mm and 24, respectively. The barrel temperature was 240 °C and the rotation speed 200 rpm. After extrusion, the extrudate was cooled in a water bath and pelletized. It is known that PA6/OMMT master-batches with large OMMT contents are not well exfoliated [4–5]. The PA6,6/PA6/OMMT nanocomposites with filler contents up to 5 wt% were obtained in the twin-screw extruder-kneader at a barrel temperature of 265 °C and a rotation speed of 60 rpm. The compositions of the PA6,6/PA6/OMMT PNs obtained were 90/9/1, 80/18/2, 70/27/3, 60/36/4 and 50/45/5. The PNs will be named by means of the OMMT content. The real clay content of the OMMT was roughly two thirds that of OMMT, as a 3 wt% nanocomposite showed a clay content of 1.95 wt% after calcination. Subsequent injection moulding was carried out in a Battenfeld BA230E reciprocating screw injection moulding machine to obtain tensile (ASTM D638, type IV, thickness 1.84 mm) and impact (ASTM D256, thickness 3.1 mm) specimens. The screw of the plasticization unit was a standard screw with a diameter of 18 mm, *L/D* ratio of 17.8 and compression ratio of 4. The melt temperature was 265 °C and the mould temperature 17 °C. The injection speed and pressure were 11.5 cm^3/s and 2300 bar, respectively.

The phase behaviour was studied both by DSC and DMTA. The DSC scans were carried out using a Perkin–Elmer DSC-7 calorimeter in a nitrogen atmosphere and using an indium sample as reference. The samples were first heated from 30 to 300 °C at 20 °C/min. Dynamic mechanical analysis was performed using a TA Q800 DMA, that provided the loss tangent (tan δ) and the storage moduli (E') against temperature. The scans were carried out in bending mode at a constant heating rate of 4 °C/min and a frequency of 1 Hz, from −10 °C to roughly 120 °C.

X-ray diffraction patterns were recorded in a Philips PW 1729 GXRD X-ray diffractometer at 45 kV and 50 mA, using a Ni-filtered Cu-K_α radiation source. The scan speed was 0.5°/min. The TEM samples were embedded and ultrathin-sectioned at 60–100 nm using an ultramicrotome (Leica, ultracut UCT). The micrographs were obtained both in an Hitachi H-7000 FA apparatus at an acceleration voltage of 125 kV and in an Hitachi 600AB apparatus at an acceleration voltage of 200 kV.

Tensile testing was carried out using an Instron 4301 machine at a cross-head speed of 10 mm/min and at 23 ± 2 °C and 50 ± 5% relative humidity. The mechanical properties (tensile strength (σ_t) and ductility, measured as the break strain (ε_b)) were determined from the load–displacement curves. The Young modulus was determined by means of an extensometer at a cross-head speed of 1 mm/min. Izod impact tests were carried out on notched specimens using a CEAST 6548/000 pendulum. The

notches (depth 2.54 mm and radius 0.25 mm) were machined after injection moulding. A minimum of five tensile specimens and 10 impact specimens were tested for each reported value.

3. Results and discussion

3.1. Characterization of the nanostructure

The characterization of the nanostructure was carried out by both XRD and TEM. In Fig. 1 the XRD plots of the OMMT, the PA6/OMMT master-batch, and the neat PA6 are shown. As can be seen, the OMMT showed a very large peak at $2\theta = 3.40°$, a very slight shoulder centred at 4.65° and a small peak at 8.00°. They corresponded by the Bragg law to basal spacing $d_{001} = 2.60$, $d_{002} = 1.90$ and $d_{003} = 1.10$ nm, respectively. The basal spacing of d_{001} and d_{002} are usual in OMMT. The basal spacing of d_{003} corresponds to unmodified MMT [29], and indicates that the inorganic cations of the smectic clay were not fully replaced by organic ions. As can also be seen, the XRD plot of the master-batch showed a wide peak centred at roughly 7° i.e. at a basal spacing of 1.26 nm that could indicate the presence of some ordered structures. However, the lack of significant deviation from neat PA6 and the disappearance of the peak of the OMMT at $2\theta = 3.40°$, indicated that the OMMT was well exfoliated in the master-batch.

In Fig. 2 the XRD plots of the PNs with 1, 2, 3, 4 and 5 wt% OMMT, and that of the OMMT as a reference are shown. As can be seen, in the PNs with 1 and 2 wt% OMMT and less clear in the case of 3 wt% OMMT, no absorption peak appeared, either at $2\theta = 3.40°$ (OMMT) or at 7° (master-batch). This indicated delamination and dispersion of the clay nanolayers, i.e. the formation of an exfoliated PA6,6-based nanostructure. Moreover, the absence of a peak at 7° (Fig. 1) indicated an exfoliation even greater than that observed in the master-batch; therefore, additional exfoliation took place during mixing of PA6,6 with the PA6/OMMT master-batch. In the PNs with 4 and 5 wt% OMMT, a weak and broad peak appeared between 1.5 and 6° (basal spacing from 5.88 to 1.47 nm) indicating the presence of intercalated nanostructures. This wide peak was not present in the master-batch (Fig. 1), indicating that as observed before [16], at high clay contents the silicate layers aggregated and/or reordered again during mixing the master-batch with PA6,6. This aggregation was less important in the case of the PN with 4 wt% OMMT, as seen because of the larger basal spacing. Fully exfoliated polymer/clay nanocomposites are difficult to obtain at high clay loadings, especially by a melt intercalation approach, because the ratio of intercalated/exfoliated nanostructures usually increases with the clay content [4–5].

It is known that the information provided by the XRD results is limited, as it gives incomplete information about the level of dispersion, and contain no peak representing delaminated OMMT [13]. For this reason, an additional analysis of the nanostructure was made by TEM. Figs. 3(a) and (b) show the TEM photomicrographs of the PNs with 1 and 3 wt% OMMT, respectively. The structure of the PNs with 2 wt% OMMT was very similar. As can be seen in Fig. 3(a), the OMMT was very highly dispersed in the matrix. The exfoliation level was higher than that observed in the PA6 master-batch. This agrees with the X-ray results and indicates that the substitution of PA6 by the majority PA6,6 in the surroundings of the OMMT layers did not produce any reverse exfoliation, but that the exfoliation degree became even higher due to the additional processing. In Fig. 3(b), a close inspection of the clay domains revealed the presence of consistent nanolayer spacing higher than 9 nm in the 3 wt% PN. This explains why no diffraction peak was observed in its XRD pattern. This is a typical characteristic of disordered and exfoliated clay nanostructures. In the case of 5 wt% OMMT PNs, individual clay platelets were predominant, but some tactoids of roughly eight sheets per stack also appeared, indicating that the nanostructure was

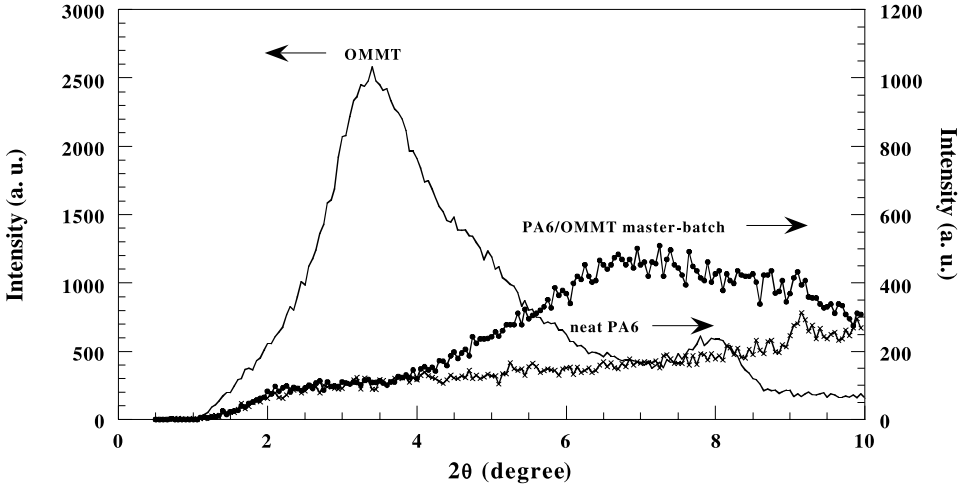

Fig. 1. X-ray diffraction patterns for OMMT, PA6/OMMT master-batch and neat PA6.

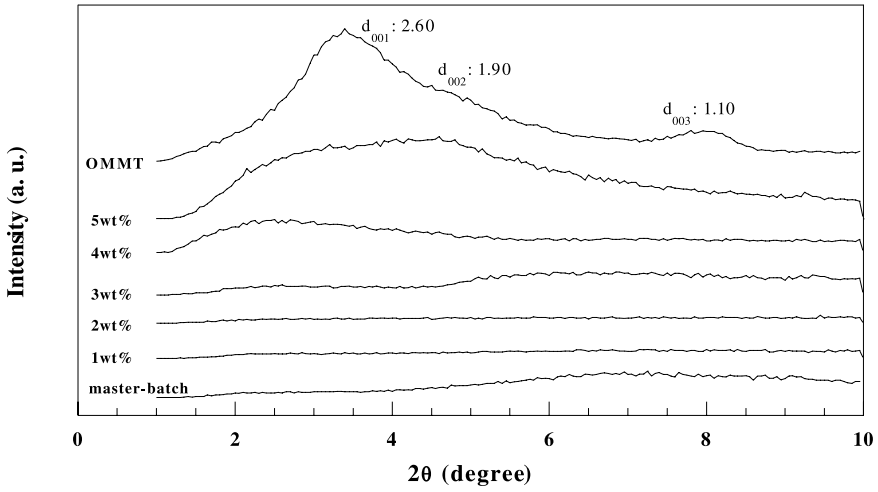

Fig. 2. X-ray diffraction patterns for OMMT and PNs with 1, 2, 3, 4 and 5 wt%.

partially exfoliated and partially intercalated. Therefore, these TEM photomicrographs confirm the results obtained by X ray diffraction.

3.2. Phase structure

The phase structure of the matrix of the PNs was studied both by DMTA and DSC. The T_gs, measured as the temperature at which the maxima in tan δ appeared, are shown as filled symbols (continuous line) in Fig. 4 against the OMMT content. As can be seen, the PNs showed only one T_g, indicating miscibility in the matrix at the PA6,6/PA6 compositions used. As can also be seen, the decrease in T_g of the PNs (continuous line) was larger as the OMMT content increased. This must be influenced by the concomitant increase in PA6 content, but the T_gs can also change due to the presence of OMMT [30]. For this reason, to find out the separate contributions of the presence of PA6 and of OMMT to the T_g change, PA6,6/PA6 binary blends were prepared under the same processing conditions as the PNs. Their T_gs were measured assuming that the presence of either PA6 or OMMT did not change their respective effect on the T_g of the PA6,6. The decreases in the T_g of PA6,6 due to the PA6 presence were subtracted from those of the PNs to calculate the effects of OMMT on T_g. The calculated T_gs should correspond to PA6,6/OMMT PNs and are plotted in Fig. 4 as empty circles.

As can be seen, no T_g change due to the OMMT presence (broken line) appeared. This was unexpected because the presence of exfoliated clay particles should lead to a decrease in the mobility of the polymer chains confined between or close to the silicate layers, and therefore to a T_g increase. This is not seen in Fig. 4 indicating that there is another parameter that influences the T_g. It is known [31] that in PNs, the presence of extra surfactant groups from the organic treatment in commercial OMMTs is usual. These extra surfactant groups remain associated with the clay after ion exchange, are not ionically bound to the surface, and taking into account their low molecular weight, they could plasticize the matrix and lead to a T_g decrease. It is assumed that this effect took place and counteracted the usual increase in the T_g of the matrix due to the presence of the clay.

The melting (T_m) and crystallization (T_c) temperatures of the PNs and of the corresponding matrices against composition are shown in Table 1. As can be seen, the PNs showed only a T_m which corresponded to PA6,6. Therefore, PA6 should be mostly amorphous. This was also seen in the case of the matrix, so that the amorphous nature of PA6 in these PNs is attributed to the much higher crystallization rate of PA6,6 that should hinder both the diffusion and the crystallization of PA6. As can also be seen, slight T_m decreases (that were also observed in T_c) were seen in the matrices at increasing PA6 contents, indicating that PA6 also hindered the crystallization of PA6,6. Finally, as seen in Table 1, the T_ms of the PA6,6/PA6 blends were similar to those of the PNs, indicating that the presence of OMMT did not affect the characteristics of the crystalline PA6,6 phase.

3.3. Mechanical properties

The tensile stress–strain curves of the PA6,6/PA6 matrices showed three necking peaks whatever the PA6 content. Two yield peaks were seen in PNs with OMMT contents up to 3 wt%. The modulus of elasticity and the yield stress of the PNs are shown respectively in Figs. 5 and 6. To find out the individual effects of PA6 and of the clay on the modulus, PA6,6/PA6 binary blends with the same PA6 contents as those of the PNs were prepared. Their modulus and yield stress are plotted as empty circles in Figs. 5 and 6.

As can be seen in Fig. 5, the modulus of elasticity of the PNs increased rather linearly upon OMMT addition. The increases were very significant, reaching 46% with respect to that of neat PA6,6 with 5 wt% OMMT content. These

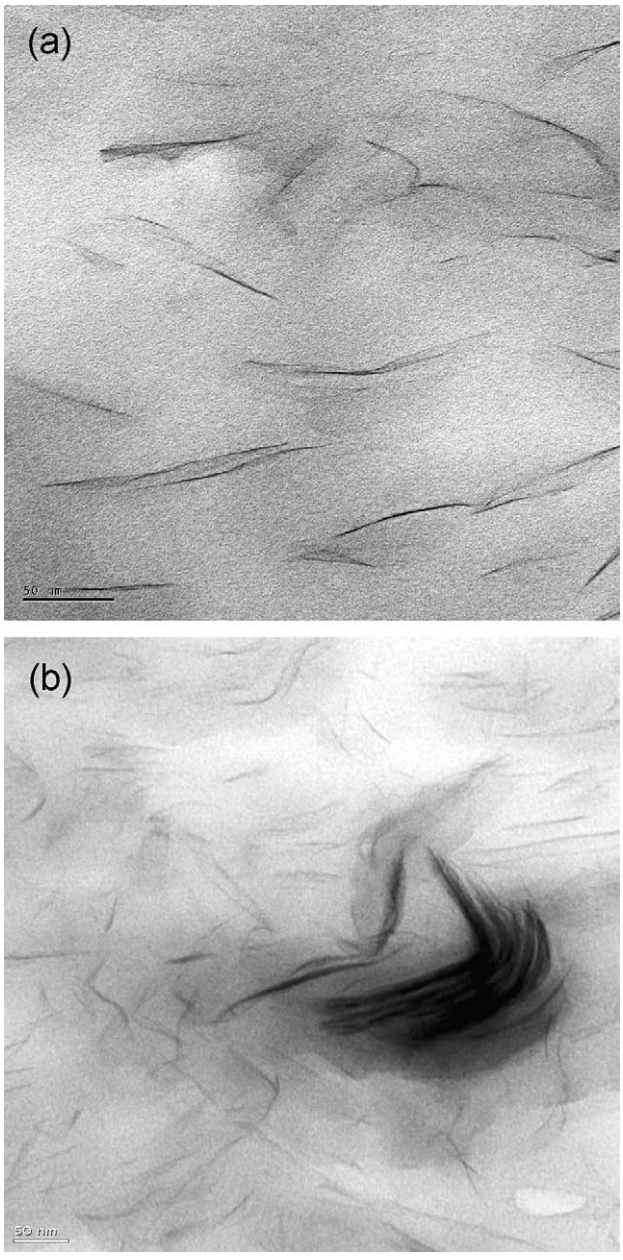

Fig. 3. TEM photomicrographs of the PNs with 1 wt% (a) and 3 wt% (b) OMMT at high magnification.

Table 1
Melting and crystallization temperatures of the PNs and their correspondent matrices against OMMT content

OMMT (%)	T_m (°C)		T_c (°C)	
	PN's	matrix	PN's	matrix
0	266	264	227	227
1	266	265	225.5	224
2	265.5	263	226.5	225.5
3	264	261	224	223
4	265.5	263	223.5	221
5	264.5	261.5	219	219

The mean typical deviation of the results was below 2%.

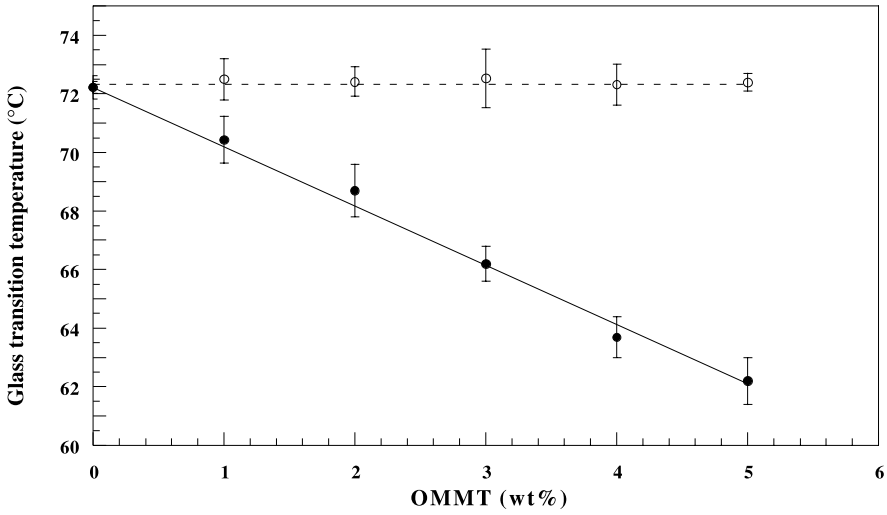

Fig. 4. Glass transition temperatures of the PNs obtained by DMTA versus OMMT content. The calculated T_gs of the PNs without PA6 appear as empty circles linked by a broken line.

increases would be larger when compared with the modulus of the matrix; this is because the increases will be smaller at larger OMMT contents due to the concomitant increasing content of the less stiff PA6. The yield stress behaved similarly to the modulus of elasticity, due to small deformation nature of both properties and increased 22% with 5 wt% OMMT content. These modulus and yield stress increases are attributed to the stiff nature of the clay filler and its high aspect ratio [23] and to the decrease in molecular mobility of the matrix, a consequence of (i) the interaction of the polymer chains with the organic modification of the OMMT content, and (ii) the large amount of interacting molecules, in its turn, a consequence of the large interphase area/dispersed volume ratio characteristic of largely exfoliated PNs. It must be mentioned that the significance of these modulus increases must be judged taking into account that the real clay content is significantly smaller (a PN with 3 wt% OMMT content had 1.95 wt% MMT) than that of plotted OMMT content.

The possible increase in the thermal resistance of the PNs was studied by means of the dynamic storage modulus (E'), that should correlate with the modulus of elasticity and is plotted against temperature in Fig. 7 for different OMMT contents. As can be seen, the percent increases in E' observed in the PNs with clay loading at room temperature (ascribed to the same reasons stated for the modulus of elasticity) were very similar to those obtained in the modulus of elasticity, indicating the relation between the two parameters. As can also be seen, the storage modulus of the PNs with OMMT contents up to 3 wt% was retained up

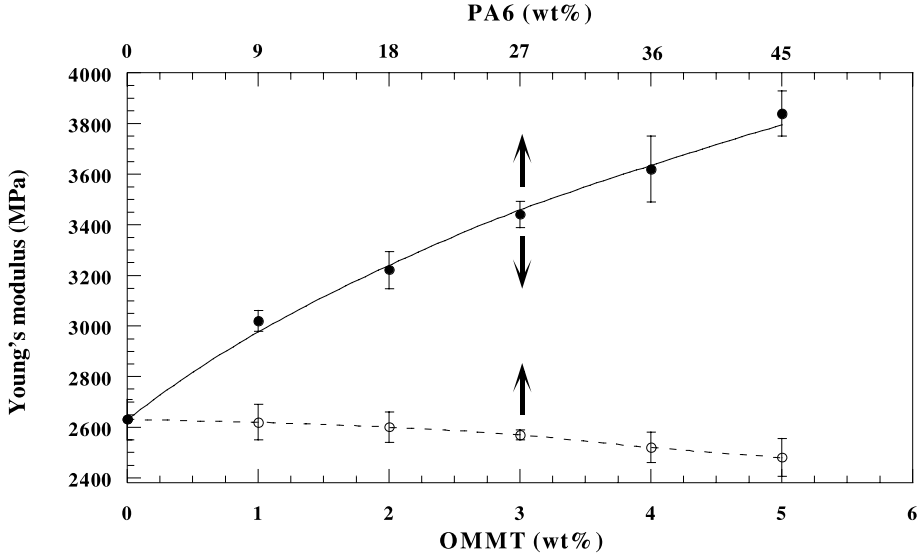

Fig. 5. Young's modulus of the PNs (full circles) versus OMMT content. The modulus of the reference PA6,6/PA6 blends are also plotted (empty circles) against the PA6 content.

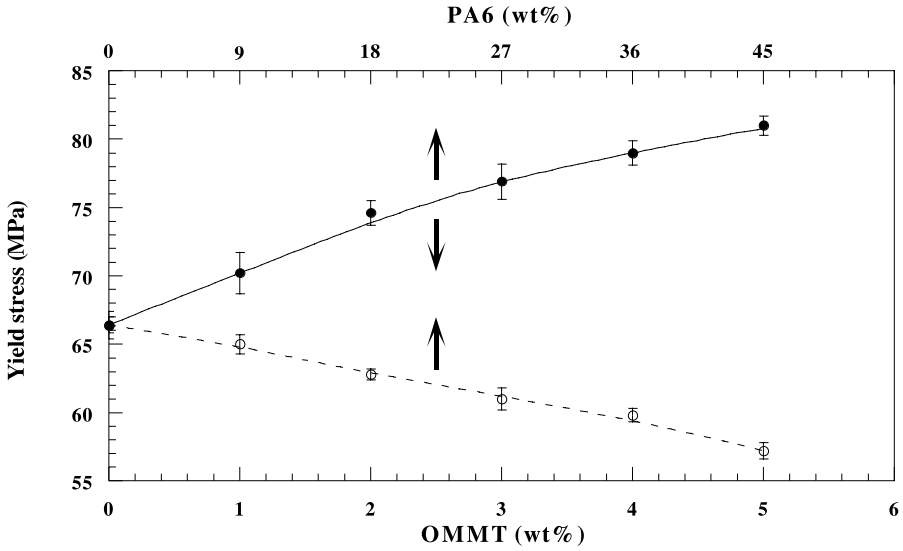

Fig. 6. Yield stress of the PNs and PA6,6/PA6 blends. Symbols as in Fig. 5.

to 40 °C, despite the increasing presence of the less thermally resistant PA6. Thus, the clay presence counteracts the smaller temperature resistance of PA6.

The ductility of the PNs measured by the elongation at break is plotted in Fig. 8 against the OMMT content. As can be seen, the ductility of the PNs decreased slightly with the OMMT content up to 3%. As expected, ductility clearly decreased in the PNs with 4 and 5 wt% OMMT, but the specimens yielded, the reduction in the area of the cross section to fracture being 7 and 6%, respectively in the 4 and 5 wt% PNs. The decrease in ductility observed in the PNs with 4 and 5 wt%, is attributed to the presence of agglomerated clay particles that were most often seen at these clay contents. The ductility decrease in the PNs of this study, for example that with 3 wt% OMMT (1.95 wt% MMT), is slightly smaller than that observed in PA6 (47%) [7] with the same MMT content, and also smaller than that observed (55%) [24] in exfoliated PA6,6, PA6 with 2.1 wt% OMMT content. These favourable ductility values could be related to the presence of excess surfactant and, more probably, to the presence of the slightly more ductile PA6. This presence of PA6, however, does not seem to have widespread negative effects, as the modulus of elasticity of the PNs that should be worsened, also showed an evident positive behaviour.

4. Conclusions

PA6 was successfully used as a mediating material to produce exfoliated PA6,6, PA6 based nanocomposites. The exfoliation of the commercial organically modified montmorillonite (OMMT) used was general up to an OMMT content of 3 wt% (1.95 wt% MMT) as seen both by X-ray

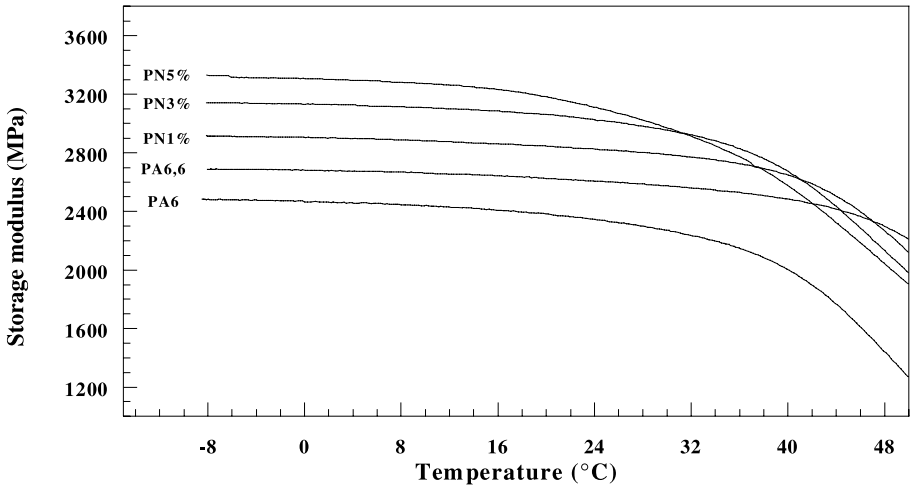

Fig. 7. Variation of dynamic storage modulus of the neat PA6,6, PA6 and PNs with 1, 3 and 5 wt% OMMT content with temperature.

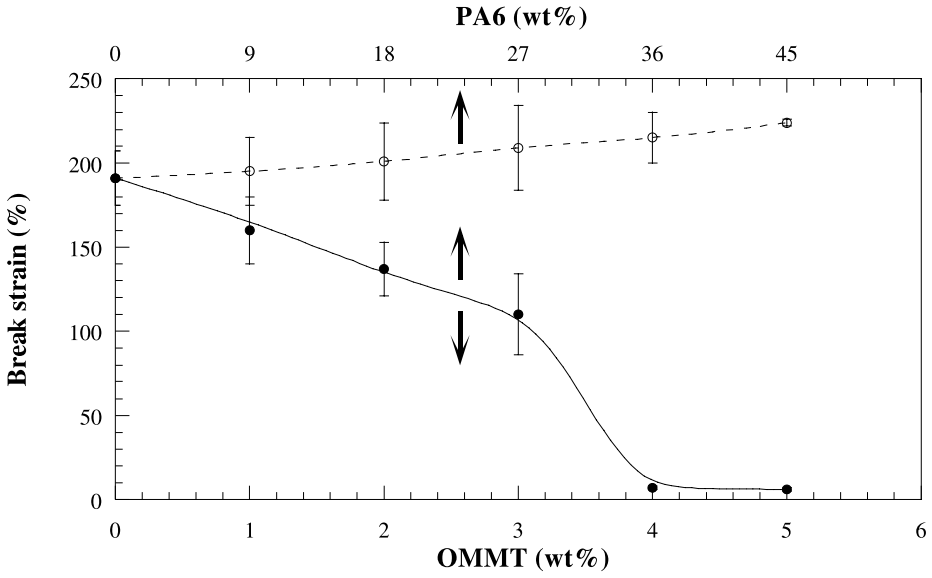

Fig. 8. Ductility of the PNs versus OMMT content.

diffraction and TEM. The slight decreases in the single T_g of the PA6,6, PA6-rich matrix were attributed to the PA6 presence. The modulus of elasticity and the yield stress increases were important and higher than those observed in other matrices. This was despite the presence of the less stiff PA6, and was attributed to the widely observed exfoliation. Ductility only slightly decreased up to 3 wt% OMMT. At higher OMMT contents it clearly decreased, due to the presence of agglomerates that, despite their sub-micron size, appear to influence ductility.

Acknowledgements

The financial support of the Basque Government (Etortek Research Program) is gratefully acknowledged. I. González thanks the Spanish Government for the award of a grant for the development of this work.

References

[1] Pinnavaia TJ, Beall GW. Polymer-clay nanocomposites. 1st ed. New York: Wiley; 2000.
[2] Liang ZM, Yin J, Xu HJ. Polymer 2003;44(5):1391–9.
[3] Lincoln DM, Vaia RA, Wang ZG, Hsiao BS, Krishnamoorti R. Polymer 2001;42(25):9975–85.
[4] Dennis HR, Hunter DL, Chang D, Kim S, White JL, Cho JW, et al. Polymer 2001;42(23):9513–22.
[5] Fornes TD, Yoon PJ, Hunter DL, Keskkula H, Paul DR. Polymer 2002;43(22):5915–33.
[6] Shah RK, Paul DR. Polymer 2004;45(9):2991–3000.
[7] Fornes TD, Hunter DL, Paul DR. Polymer 2004;45(7):2321–31.
[8] Fornes TD, Hunter DL, Paul DR. Macromolecules 2004;37(5):1793–8.
[9] Pantoustier N, Lepoittevin B, Alexandre M, Kubies D, Calberg C, Jérôme R, et al. Polym Eng Sci 2002;42(9):1928–36.
[10] Lepoittevin B, Devalckenaere M, Pantoustier N, Alexandre M, Kubies D, Calberg C, et al. Polymer 2002;43(14):4017–23.
[11] Su S, Wilkie CA. J Polym Sci; Part A: Polym Chem 2003;41(8):1124–35.
[12] Li X, Kang T, Cho WJ, Lee JK, Ha CS. Macromol Rapid Comm. 2001;22(16):1306–12.
[13] Davis CH, Gilman J, Schiraldi JW, Shields DA, Randy J. J Polym Sci, Part B: Polym Phys 2002;40(23):2661–6.
[14] Nam PH, Maiti P, Okamoto M, Kotada T, Hasekawa N, Usuki A. Polymer 2001;42(23):9633–40.
[15] Gonzalez I, Eguiazabal JI, Nazabal J. to be published.
[16] Kim SW, Jo WH, Lee MS, Ko MB, Jho JY. Polymer 2001;42(24):9837–42.
[17] Lepoittevin B, Pantoustier N, Devalckenaere M, Alexandre M, Calberg C, Jérôme R, et al. Polymer 2003;44(7):2033–40.
[18] Liu X, Wu Q, Berglund LA. Polymer 2002;43(18):4967–72.
[19] Liu X, Wu Q, Zhang Q, Mo Z. J Polym Sci Part B: Polym Phys 2003;41(1):63–7.
[20] Yu ZZ, Yang M, Zhang Q, Zhao C, Mai YW. J Polym Sci, Part B: Polym Phys 2003;41(11):1234–43.
[21] Nair SV, Goettler LA, Lysek BA. Polym Eng Sci 2002;42(9):1872–82.
[22] Tanaka G, Goettler LA. Polymer 2002;43(2):541–53.
[23] Liu X, Wu Q. Macromol Mater Eng 2002;287(3):180–6.
[24] Han B, Ji G, Wu S, Shen J. Eur Polym J 2003;39(8):1641–6.
[25] Zhu CS, Kang X, He SQ, Wang LY, Lu LY. Chinese J Polym Sci 2002;20(6):551–7.
[26] Dharaiya D, Jana SC, Shafi A. Polym Eng Sci 2003;43(3):580–95.
[27] Lee MS, Ha MG, Choi CN, Yang KS, Kim JB, Choi GD. Polym J 2002;34(7):510–4.
[28] Rybnikár F, Geil PH. J Appl Polym Sci 1993;49(7):1175–88.
[29] Chang JH, Park KM, Cho D. Polym Eng Sci 2001;41(9):1514–20.
[30] Chang JH, Seo BS, Hwang DH. Polymer 2002;43(10):2969–74.
[31] Morgan AB, Harris JD. Polymer 2003;44(8):2313–20.